Experimental verification of the IPI sizing technique

Sebastian Kosch

July 2014

Introduction

1.1 Why spray sizing is important

1.2 What our contributions in this paper are

- Our contributions: - Pupillary magnification has to be taken into account - Circle detection algorithm is crap

1.3 What other work has been done in this area

Experimental setup

- Our setup:

2.1 Dantec system

- Dantec system

2.2 PDPA system

- TSI system

2.3 Droplet generator

- Droplet generator

2.4 Verification of droplet sizes

- This is where I show pictures and tables, showing that the formula actually works.

Interferometric Particle Imaging

3.1 Operating principle

The number of fringes N_{fr} appearing in the image has a simple linear relationship to the droplet diametre D_d:

$$N_{\text{fr}} = \varkappa D_d, \tag{3.1}$$

where $\varkappa$ is a constant derived from the optical configuration:

$$\varkappa = \frac{\arcsin\left(\frac{D_a}{2z}\right)}{\lambda}\left(\cos\frac{\varphi}{2} - \frac{m\sin\frac{\varphi}{2}}{\sqrt{m^2+1-2m\cos\frac{\varphi}{2}}}\right). \tag{3.2}$$

In the above expression D_a is the aperture diametre, z is the distance of the lens to the laser sheet, φ is the off-axis angle (90 degrees in most setups, including ours), and m is the relative refractive index of the droplets (1.333 for water in air).

3.2 Setup

(How it's set up, what cameras, what lenses, what laser, timer box, software, etc.)

3.3 Common problems and sources of error

3.3.1 Too much overlap

This is a section where I refer to the paper that calculates overlap probabilities. I explain that many droplets are mis-identified (either high-freq is seen as low-freq, or noise is seen as high-freq) and where I point out that while Hanning windows and min-distance/max-overlap filters help a little bit, they also skew the representativeness of the sample because only small, dispersed satellites are outside of the main flow.

Figure 3.1: Overlapping defocussed droplet images

I explain that there isn't really an easy method of fixing this, and that any time spent attempting to deal with the problem is better spent building a slit aperture system, as described in the next chapter.

3.3.2 Droplet detection and camera mapping

The most challenging stage of the measurement process is the detection of the defocussed droplet images. Since the defocussed images assume the shape of the aperture, which is wide open in most applications,[1] they are typically circular. Moreover, they are all more or less of the same size as a consequence of equation (??).

It thus stands to reason that a simple circle detection technique would suffice to detect the droplet images in the photos. A polar adaptation of the Hough accumulator technique (such as the OpenCV implementation `cv2.HoughCircles()`) or a correlation-based pattern matching method (e.g. `cv2.matchTemplate()`) are both obvious choices for this task. The problem of *droplet overlap*, however, can thwart such efforts (Figure 3.1). This happens particularly when large droplets are to be measured, because their many fringes require larger defocussed images to resolve clearly. Indeed, in regions of high droplet density, it can be impossible to reliably detect the circular fringe images using the methods mentioned above.

Nevertheless, once droplet image positions are established with confidence, overlap can be dealt with to a degree: known overlapping regions can either be excluded entirely or serve to help find maximum-likelihood frequency peaks for their respective tributary droplet images.

Since the detection of droplet images is so essential, the Dantec DynamicStudio software extracts the droplets' positions from the focussed photo, and then maps those positions onto the defocussed photo based on a set of camera calibration photos. This method is sound in principle, but often yields unsatisfactory mappings in practice, likely whenever the calibration target plate (Figure ??) is not precisely aligned with the laser sheet. In section ??, we describe a more accurate and robust method of finding the mapping based directly on the pair of droplet photos.

Since the mapping error is often a perspectivity, the simple manual x/y-shift that can be applied in the DynamicStudio software after calibration is not a sufficient adjustment.

Dantec supplies a *standard dot target*, a white $10 \times 10\,\mathrm{cm}^2$ plate engraved with a pattern of black dots (Figure ??). The plate is to be mounted such that its surface coincides perfectly with the laser sheet. Both cameras are then focussed on the dot pattern, and a photo is taken with both. This allows the DynamicStudio software to calculate the transformation matrix

[1] see Chapter ?? for a discussion of the benefits of non-circular apertures.

between target plate and image for each camera:

$$\begin{bmatrix} x' \\ y' \\ z' \\ r' \end{bmatrix} = \begin{bmatrix} S_x & A_{yx} & A_{zx} & T_x \\ A_{xy} & S_y & A_{zy} & T_y \\ A_{xz} & A_{xy} & S_z & T_z \\ P_x & P_y & P_z & S_0 \end{bmatrix} \begin{bmatrix} x \\ y \\ z \\ 1 \end{bmatrix}. \tag{3.3}$$

In practice, $P_{x,y,z} = 0$ and $S_z = S_0 = 1$, such that the mapping is affine (although we will later show that this need not be the case). The z-components (third row/column) are ignored, such that a 3×3 matrix suffices for the purposes of this discussion:

$$\begin{bmatrix} x' \\ y' \\ r' \end{bmatrix} = \begin{bmatrix} S_x & A_{yx} & T_x \\ A_{xy} & S_y & T_y \\ P_x & P_y & S_0 \end{bmatrix} \begin{bmatrix} x \\ y \\ 1 \end{bmatrix}. \tag{3.4}$$

The DynamicStudio software thus finds the camera matrices $\mathbf{P}_{\text{foc}}$ and $\mathbf{P}_{\text{def}}$ mapping the object (the target plate) onto the two camera images:[2]

$$\mathbf{x}'_{\text{foc}} = \mathbf{P}_{\text{foc}}\,\mathbf{x} \tag{3.5}$$

$$\mathbf{x}'_{\text{def}} = \mathbf{P}_{\text{def}}\,\mathbf{x}. \tag{3.6}$$

It follows that the quotient of the two matrices, also known as the homography

$$\mathbf{H} = \mathbf{P}_{\text{def}}\,\mathbf{P}_{\text{foc}} \tag{3.7}$$

can be used to map the focussed image onto the defocussed image:

$$\mathbf{H}\,\mathbf{x}'_{\text{foc}} = \mathbf{x}'_{\text{def}}. \tag{3.8}$$

In practice, it is not always possible to ensure that the dot target plate is aligned with the laser light sheet to absolute perfection. This introduces a perspective error in the homography matrix $\mathbf{H}$. Figure 3.2a shows that even though the calibration images are mapped perfectly, there is a perspective error in Figure 3.2b.

To correct for this error, we can use image registration techniques to derive the homography mapping *directly* from the focussed and defocussed droplet images, doing away with the need for calibration pictures altogether. Once we find the corrected homography $\hat{\mathbf{H}}$, we use it to find

$$\hat{\mathbf{P}}_{\text{def}} = \hat{\mathbf{H}}\,\mathbf{P}_{\text{foc}}, \tag{3.9}$$

which can be manually entered into the DynamicStudio software to replace $\mathbf{P}_{\text{def}}$.

Finding the corrected homography

Image registration is the process of finding the best possible mapping of one image onto another – in other words, it is a term for homography-finding techniques. The basic process comprises three steps:

[2] Henceforth, the subscripts "foc" and "def" shall designate the focussed and defocussed cameras, respectively – even though both are focussed when the initial calibration photo is taken.

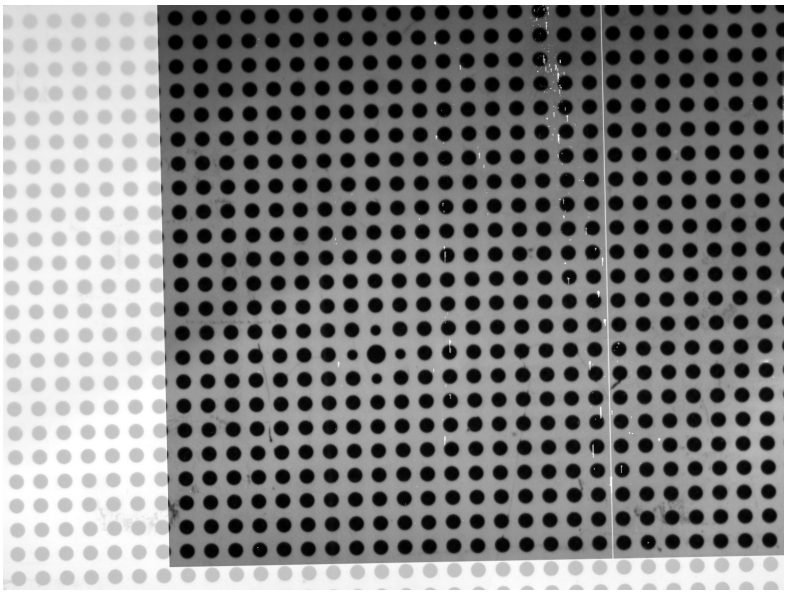

(a) Focussed camera image, after applying homography, is superimposed onto defocussed camera image of dot target plate.

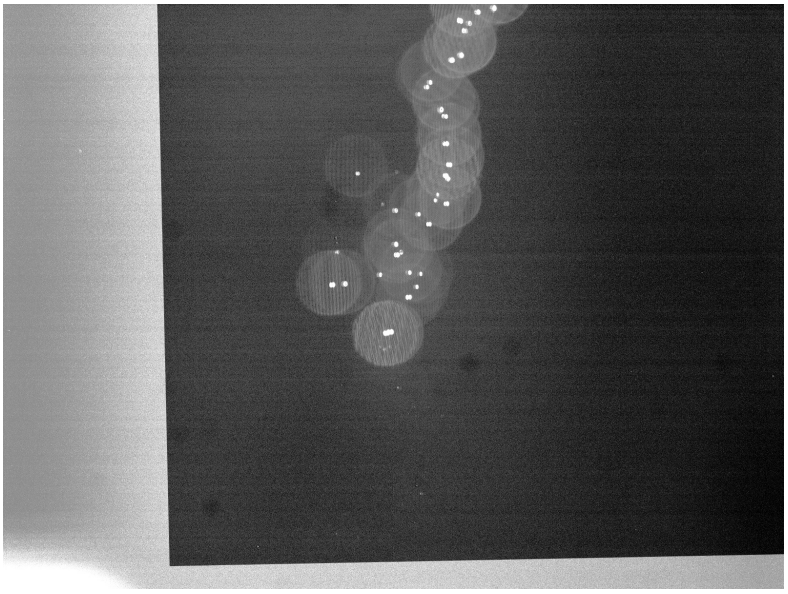

(b) Focussed camera image, after applying homography derived from the calibration images, is superimposed onto defocussed camera image of droplets.

Figure 3.2: Illustration of the perspective error from misaligned calibration target plate

1. **Feature detection:** Finding "features", i.e. unique points or regions in the images – such as corners, arcs, or contrasting regions which stay relatively stable even when the image is thresholded.

2. **Feature description:** Converting the detected features into numerical vectors.

3. **Feature matching:** Finding good correspondences between features in the two images – this often requires inlier/outlier decision-making, e.g. RANSAC.

Naturally, image registration is impossible to achieve between our focussed and defocussed images. We therefore first apply the following steps to our focussed image:

1. Mask the image, excluding all areas that are known not to contain droplets.

2. Subtract the pixel-wise minimum or mean taken over all images taken by the camera. This step will remove hot pixels on the camera's CCD sensor and other static noise.

3. Erode the image, using a 3×3 or 5×5 kernel. This will close any remaining bright pixels which are likely noise.

4. Locate the intensity peaks in the remaining image.

5. Fill a new image with black, then draw white circles of diameter D_d onto it, centered at the respective positions of the intensity peaks detected in the focussed image.

The result of these operations is shown in Figure 3.3.

Image registration algorithms are often not very robust. This is especially true when the two pictures are not photos taken from slightly different angles. Moreover, image processing algorithms have runtime complexities that grow at least with the area of the image. We therefore prepare our focussed image by shrinking it to half the size (transformation $\mathbf{S}_{0.5}$) and mirroring it horizontally (transformation $\mathbf{M}_h$).

Our image registration algorithm makes use of the affine invariance of the ASIFT algorithm [], but instead of the patented SIFT detector/descriptor pair [], we use ORB [] for feature detection and BRIEF [] for feature description. A more detailed explanation of the algorithm can be found in Appendix **??**. Figure 3.4 shows a successful mapping between focussed and defocussed images.

The homography found by the registration algorithm, $\mathbf{K}$, must now be converted into a homography between the original images, $\hat{\mathbf{H}}$. We see that

$$\mathbf{K}\,\mathbf{M}_h\,\mathbf{S}_{0.5}\,\mathbf{P}_{\text{foc}} = \mathbf{S}_{0.5}\mathbf{P}_{\text{def}}; \tag{3.10}$$

note here that the mirroring operation is applied only on one side of the equation, since the original images are mirrored and the goal is to undo this before running the image registration. To bring this into the form required by (3.8), we write

$$\mathbf{S}_{0.5}^{-1}\,\mathbf{K}\,\mathbf{M}_h\,\mathbf{S}_{0.5}\,\mathbf{P}_{\text{foc}} = \mathbf{S}_{0.5}^{-1}\,\mathbf{S}_{0.5}\mathbf{P}_{\text{def}} \tag{3.11}$$

$$= \mathbf{P}_{\text{def}} \tag{3.12}$$

(a) Focussed camera image.

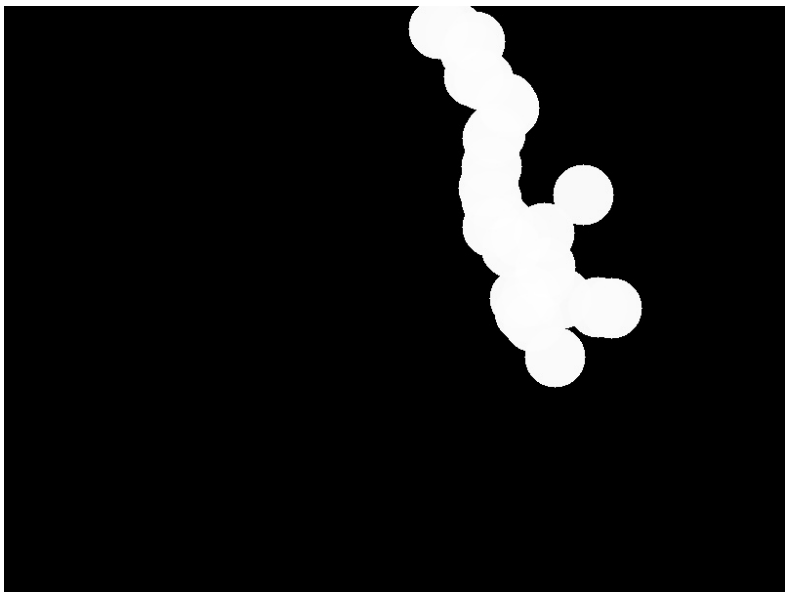

(b) Simulated defocussed camera image based on focussed camera image, used for registration.

Figure 3.3: Using the focussed image to simulate the defocussed image for registration

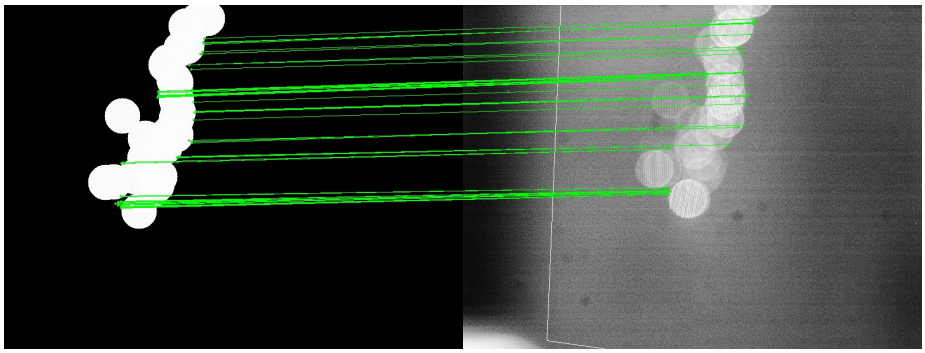

Figure 3.4: Matching between focussed and defocussed images.

Finally, it turns out that DynamicStudio violates convention by placing the coordinate origin at the bottom left corner of the image. We must therefore pre- and post-multiply by $\mathbf{M}_v^{\pm 1}$ to arrive at our final expression for $\hat{\mathbf{H}}$:

$$\hat{\mathbf{H}} = \mathbf{M}_v \, \mathbf{S}_{0.5}^{-1} \, \mathbf{K} \, \mathbf{M}_h \, \mathbf{S}_{0.5} \, \mathbf{M}_v^{-1}. \tag{3.13}$$

We shall provide the transformation matrices for convenience:

$$\mathbf{M}_h = \begin{bmatrix} -1 & 0 & \text{(image width)} \\ 0 & 1 & 0 \\ 0 & 0 & 1 \end{bmatrix} \tag{3.14}$$

$$\mathbf{M}_v = \begin{bmatrix} 1 & 0 & 0 \\ 0 & -1 & \text{(image height)} \\ 0 & 0 & 1 \end{bmatrix} \tag{3.15}$$

$$\mathbf{S}_{0.5} = \begin{bmatrix} 0.5 & 0 & 0 \\ 0 & 0.5 & 0 \\ 0 & 0 & 1 \end{bmatrix} \tag{3.16}$$

The improved matching achieved using $\hat{\mathbf{P}}_{\text{def}}$ is shown in Figure 3.5. Having calculated $\hat{\mathbf{P}}_{\text{def}}$ using equation (3.9), we can import it into DynamicStudio to improve the identification of droplets.

3.4 Thin lens assumption

What matters is the Numerical Aperture (NA), which is (the sine of half of) the collection angle. When we have a simple lens, we can calculate this as

$$\text{NA} = \sin \frac{d_a}{2z} 3\alpha\rho = \sqrt{2\lambda x r} \tag{3.17}$$

The Dantec manual suggests using the distance from light sheet to front of the lens for z, and the ratio of min focal length and max f-number to find d_a. This, however, does not result in an accurate value for the collection angle with all lenses.

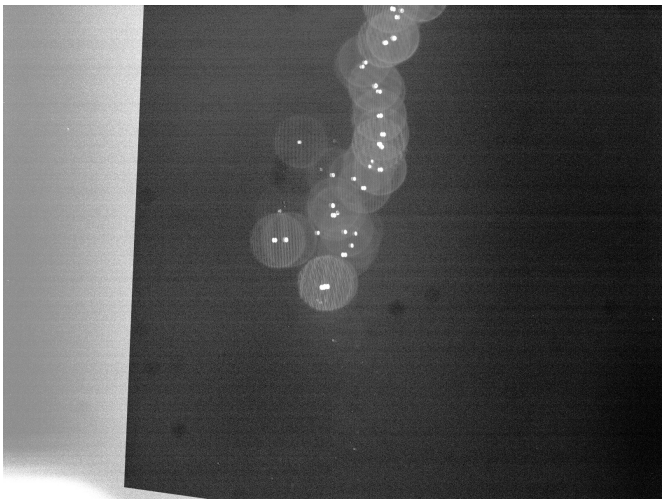

Figure 3.5: Focussed camera image, after applying homography derived from image registration, is superimposed onto defocussed camera image of droplets.

We are assuming, then, that the effective aperture (the entrance pupil) always stays constant throughout the focussing range of the lens. This is not necessarily the case, as there are lenses which change both the physical and the virtual size of the aperture when focussing. The best way to get the collecting angle is to go by magnification

3.4.1 Finding the correct value for aperture diameter

Here is where I make the claim that it is impossible to determine the actual exact value for the numerical aperture of the lens. Similarly, it can be quite difficult to determine the accurate distance from light sheet to lens aperture (even though the latter measurement is more forgiving, since the distances are far greater).

3.4.2 Error in the Mie approximation at small sizes

As outlined in paper ... geometric optics deviate from the true Mie scattering field when sizes are very small.

Global particle sizing with a slit aperture

To ensure that no systemic problems are introduced by our setup, we performed the experiment after installing a slit aperture over the camera lens. This well-known and reliable technique was first introduced by X [**?**] and is part of several commercial systems today. The aperture pares off the top and bottom halves of the defocused circles, leaving only a narrow center strip in the middle, which nonetheless covers all the fringes. This improvement, shown in Figure 4.1, overcomes the problem of overlapping circles.

4.1 Optical theory

This is where I explain the relationship between slit size and position, and size and position of the measured strips.

4.2 Image processing

Extracting the fringe counts from such an image is straightforward. First, we correlate the image with that of a single bright strip, resulting in intensity peaks centered over our regions of interest (Figure **??**). We then apply a horizontal Hanning window to each of those regions and feed them through a Fourier transform, with typical results as shown in Figure **??**. If the frequency peak exceeds the average value by some threshold amount (here: 37%), it is turned into a fringe count by re-scaling it to the size of the defocused circle. The fringe counts are then changed into droplet diameters by equation (3.2).

This needs to be explained a little more.

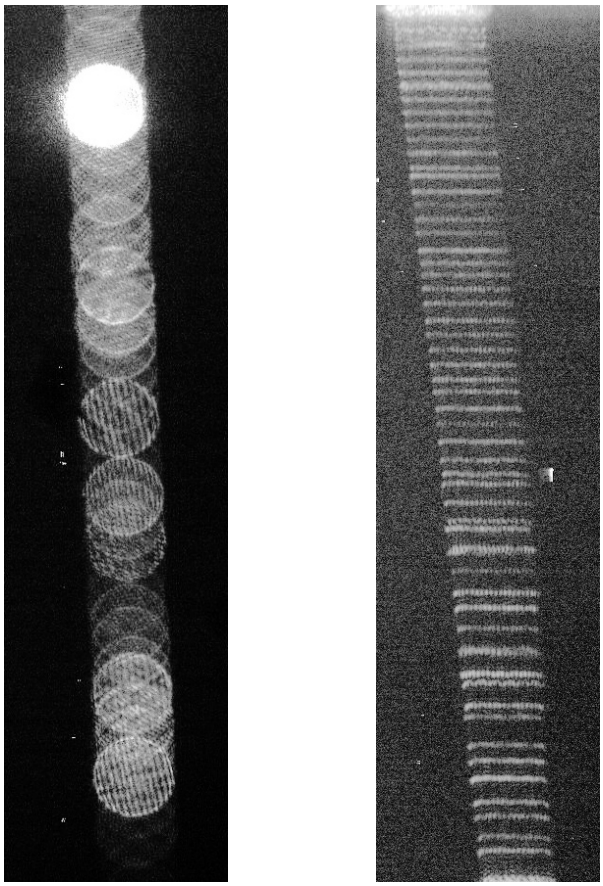

(a) (b)

Figure 4.1: Before (a) and after (b) installing the slit aperture

4.3 Sources of error with the slit method

4.3.1 Is the slit centered with respect to the droplets?

While we will get the right frequency, we might not get the right defocussed droplet size. It may therefore happen that we get the wrong final fringe count. With a circular defocussed image, it is relatively easy to approximate the mean defocussed diameter; with a line it is impossible to tell whether we are getting a cropped image of the center of the circle or one from above (show image).

While this can be remedied to some extent when applying the mask and setting up the camera position (preview the image in the software, maximize diameter), it's not very exact, and it's easy to miss a fringe. This will, of course, typically result in fringes being missed, and thus the droplets being reported as smaller than they are in reality.

4.4 Calibrating the slit method

Taking into account the sources of errors explained in the sections above, it is advisable to run a few calibration tests with droplets of different sizes before employing the IPI technique for real spray measurements. Recall that, if we ignore the Mie error, the relationship between fringe count and droplet diameter is linear with a constant of proportionality χ (see equation (3.2)). The expression for χ itself is linear in the value for numerical aperture. Finally, a badly aligned slit will reduce the number of fringes counted in a predictably linear fashion. We should therefore be able to introduce a simple correction factor once we have calibrated the device.

4.4.1 A sample calibration of the slit aperture method

Here is where I post my examples.

4.5 Discussion of Results

This is where I list my results and discuss what they might mean for calibration purposes.

4.6 Conclusion

- Conclusion: - Dantec's circle detection algorithm is garbage - Use a slit aperture instead

Phase-Doppler Particle Analysis

This is on PDPA method.